The Journal of Immunology

Endothelial Pannexin 1 Channels Control Inflammation by Regulating Intracellular Calcium

Yang Yang, Leon J. Delalio, Angela K. Best, Edgar Macal, Jenna Milstein, Iona Donnelly, Ashley M. Miller, Martin McBride, Xiaohong Shu, Michael Koval, Brant E. Isakson and Scott R. Johnstone

J Immunol published online 20 April 2020
http://www.jimmunol.org/content/early/2020/04/17/jimmunol.1901089

This information is current as of April 21, 2020.

Supplementary Material **http://www.jimmunol.org/content/suppl/2020/04/17/jimmunol.1901089.DCSupplemental**

Why *The JI*? Submit online.

- **Rapid Reviews! 30 days*** from submission to initial decision
- **No Triage!** Every submission reviewed by practicing scientists
- **Fast Publication!** 4 weeks from acceptance to publication

**average*

Subscription Information about subscribing to *The Journal of Immunology* is online at: http://jimmunol.org/subscription

Permissions Submit copyright permission requests at: http://www.aai.org/About/Publications/JI/copyright.html

Email Alerts Receive free email-alerts when new articles cite this article. Sign up at: http://jimmunol.org/alerts

The Journal of Immunology is published twice each month by The American Association of Immunologists, Inc., 1451 Rockville Pike, Suite 650, Rockville, MD 20852
Copyright © 2020 by The American Association of Immunologists, Inc. All rights reserved.
Print ISSN: 0022-1767 Online ISSN: 1550-6606.

Downloaded from http://www.jimmunol.org/ at Cochin Univ Biblio I894 on April 21, 2020

Published April 20, 2020, doi:10.4049/jimmunol.1901089

Endothelial Pannexin 1 Channels Control Inflammation by Regulating Intracellular Calcium

Yang Yang,*,† Leon J. Delalio,* Angela K. Best,* Edgar Macal,* Jenna Milstein,* Iona Donnelly,‡ Ashley M. Miller,‡ Martin McBride,‡ Xiaohong Shu,† Michael Koval,§,¶ Brant E. Isakson,*,‖ and Scott R. Johnstone*

The proinflammatory cytokine IL-1β is a significant risk factor in cardiovascular disease that can be targeted to reduce major cardiovascular events. IL-1β expression and release are tightly controlled by changes in intracellular Ca^{2+} ($[Ca^{2+}]_i$), which has been associated with ATP release and purinergic signaling. Despite this, the mechanisms that regulate these changes have not been identified. The pannexin 1 (Panx1) channels have canonically been implicated in ATP release, especially during inflammation. We examined Panx1 in human umbilical vein endothelial cells following treatment with the proinflammatory cytokine TNF-α. Analysis by whole transcriptome sequencing and immunoblot identified a dramatic increase in Panx1 mRNA and protein expression that is regulated in an NF-κB–dependent manner. Furthermore, genetic inhibition of Panx1 reduced the expression and release of IL-1β. We initially hypothesized that increased Panx1-mediated ATP release acted in a paracrine fashion to control cytokine expression. However, our data demonstrate that IL-1β expression was not altered after direct ATP stimulation in human umbilical vein endothelial cells. Because Panx1 forms a large pore channel, we hypothesized it may permit Ca^{2+} diffusion into the cell to regulate IL-1β. High-throughput flow cytometric analysis demonstrated that TNF-α treatments lead to elevated $[Ca^{2+}]_i$, corresponding with Panx1 membrane localization. Genetic or pharmacological inhibition of Panx1 reduced TNF-α–associated increases in $[Ca^{2+}]_i$, blocked phosphorylation of the NF-κB–p65 protein, and reduced IL-1β transcription. Taken together, the data in our study provide the first evidence, to our knowledge, that $[Ca^{2+}]_i$ regulation via the Panx1 channel induces a feed-forward effect on NF-κB to regulate IL-1β synthesis and release in endothelium during inflammation. ***The Journal of Immunology*****, 2020, 204: 000–000.**

Sustained inflammatory responses critically regulate the pathogenesis of endothelial dysfunction and atherosclerosis (1, 2). The release of TNF-α enhances inflammation in atherosclerosis, and TNF-α concentrations are associated with an elevated risk of atherothrombosis and the resulting major adverse cardiovascular events (3–5). Whereas many studies have focused on the effect of TNF-α on inflammatory cells (6), TNF-α has also been shown to induce production of proinflammatory cytokines in endothelial cells (ECs) (7, 8). In the presence of TNF-α, ECs synthesize and release proinflammatory cytokines and chemokines that enhance the inflammatory response, correlating with a high risk of vascular injury (8, 9). Targeting inflammation (e.g., using TNF-α antagonists) leads to reductions in cytokine expression by ECs and can reduce atherosclerotic lesion formation (10–13). Thus, defining critical EC signaling pathways may help identify therapeutic targets. Among these potential targets, IL-1β is widely considered to be a highly active and essential regulator of the pathogenesis of human atherosclerotic disease progression and susceptibility to atherothrombosis (14). Therapeutically targeting IL-1β decreases its activity and is associated

*Robert M. Berne Cardiovascular Research Center, University of Virginia School of Medicine, Charlottesville, VA 22908; †Department of Pharmacology, Dalian Medical University, Dalian 116044, China; ‡British Heart Foundation Cardiovascular Research Centre, College of Medical, Veterinary and Life Sciences, University of Glasgow, Glasgow G12 8TA, United Kingdom; §Division of Pulmonary, Allergy, Critical Care and Sleep Medicine, Department of Medicine, Emory University School of Medicine, Atlanta, GA 30322; ¶Department of Cell Biology, Emory University School of Medicine, Atlanta, GA 30322; and ‖Department of Molecular Physiology and Biophysics, University of Virginia School of Medicine, Charlottesville, VA 22908

ORCIDs: 0000-0002-0314-8049 (J.M.); 0000-0002-9794-5347 (I.D.); 0000-0003-0299-1963 (X.S.); 0000-0002-5422-5614 (M.K.); 0000-0002-7692-6294 (B.E.I.); 0000-0003-1920-5033 (S.R.J.).

Received for publication September 10, 2019. Accepted for publication March 27, 2020.

This work was supported by National Institutes of Health Grants HL120840 (to B.E.I.) and HL137112 (to B.E.I. and M.K.), China Scholarship Council (CSC) Award 201708210238 (to Y.Y.), an American Heart Association Career Development Award (19CDA34630036) (to S.R.J.), a Lord Kelvin Adam Smith Research Fellowship from the University of Glasgow (to S.R.J.), and the Welcome Trust Institutional Strategic Support Fund (University of Glasgow) (to S.R.J.).

S.R.J., B.E.I., and M.K. conceived this study, conceptualized, and provided financial backing. S.R.J. and Y.Y. designed and executed the majority of the experiments. L.J.D., A.K.B., E.M., and J.M. performed extensive cell culture and immunoblotting. A.M.M. and I.D. designed and performed RNA analysis for RNA-seq. M.M. performed RNA-seq data analysis. Y.Y. wrote the manuscript with input from X.S., M.K., B.E.I., and S.R.J.

The RNA-sequencing data presented in this article have been submitted to the European Molecular Biology Laboratory–European Bioinformatics Institute ArrayExpress (https://www.ebi.ac.uk/arrayexpress/) under accession number E-MTAB-8299.

Address correspondence and reprint requests to Prof. Brant E. Isakson, Robert M. Berne Cardiovascular Research Center, University of Virginia School of Medicine, 409 Lane Road, MR4 Building, Room 6071, Charlottesville, VA 22908 or Dr. Scott R. Johnstone at the current address: Fralin Biomedical Research Institute at Virginia Tech Carilion, Roanoke, Virginia, VA 24016. E-mail addresses: brant@virginia.edu (B.E.I.) or scottrj@vt.edu (S.R.J.)

The online version of this article contains supplemental material.

Abbreviations used in this article: AM, acetoxymethyl ester; $[Ca2^+]_i$, intracellular Ca^{2+}; CHX, cycloheximide; CT, cycle threshold; 2^-ΔΔCT, δ-δ CT; EC, endothelial cell; HPSS, HEPES physiological salt solution; M200, Medium 200; 0.1%-M200, M200 with Low Serum Growth Kit and 0.1% FBS; Panx1, pannexin 1; Panx1-Gly, Panx1-glycosylation; pmeLUC, plasma membrane luciferase; p-p65, phosphorylation of the NF-κB protein p65; PxIL2P, pannexin intracellular loop 2 peptide; qRT-PCR, quantitative RT-PCR; RNA-seq, RNA sequencing; siControl, control siRNA; siPanx1, siRNA targeting the human PANX1 gene; siRNA, silencing RNA; SMC, smooth muscle cell; THP1, Th precursor 1.

Copyright © 2020 by The American Association of Immunologists, Inc. 0022-1767/20/$37.50

Downloaded from http://www.jimmunol.org/ at Cochin Univ Biblio I894 on April 21, 2020

with a reduced expression of multiple proinflammatory cytokines, including IL-6, which have been implicated as a potential causal pathway for atherosclerotic events (15, 16). In the recent Canakinumab Anti-inflammatory Thrombosis Outcome Study, IL-1β neutralization by canakinumab reduced inflammation and decreased major adverse cardiovascular events associated with atherothrombosis in high-risk patients (14, 16). Whereas other proinflammatory cytokines, such as IL-6, have been implicated in atherosclerosis, clinical trials targeting this did not result in marked improvements in patient risk, highlighting the importance of targeting specific proinflammatory markers (17, 18). The efficacy of specific IL-1β blockade in inflammation highlights the need to elucidate the molecular mechanisms that regulate its synthesis and release.

ATP is increasingly recognized as an important factor in the regulation of the inflammatory process, leading to activation of the inflammasome (19–21). Multiple studies have now demonstrated an association between ATP release and increases in IL-1β synthesis and release (22, 23). Although some studies suggest that ATP alone is capable of increasing IL-1β synthesis and release (22), a "two-signal" model of production followed by later activation has been extensively described for IL-1β (23, 24). Priming "signal 1" activation occurs through molecules, such as TNF-α, which induce the production of pro–IL-1β through NF-κB signaling. This is followed by "signal 2" mechanisms regulated by pathogen-associated molecular patterns and damage-associated molecular patterns that promote activation of NLRP inflammasome, which enhances the magnitude and velocity of posttranslational processing of pro–IL-1β, yielding the bioactive molecule, which is released into the extracellular space (24, 25). In this model, under noninfectious conditions, ATP is suggested to act as a signal 2 mechanism (25). However, many of these studies have required the use of nonphysiological levels of ATP in the micromolar range, which has led to the suggestion that ATP is producing cytotoxic effects in cells, although this has been further debated (24, 26). Release of ATP from cells can signal locally through paracrine receptors (e.g., P2X7) to promote K^+ release leading to uptake of extracellular Ca^{2+}, which is associated with an increase in the expression and release of cytokines, including IL-1β (27–29). Further data suggest that chelation of intracellular Ca^{2+} ($[Ca^{2+}]_i$) inhibits the processing and release of IL-1β, suggesting that an influx of extracellular Ca^{2+} is centrally linked to IL-1β production (30, 31). Despite this, the source and regulation of increased $[Ca^{2+}]_i$ has not been rigorously defined (30, 31).

Pannexin 1 (Panx1) forms large, nonselective plasma membrane channels that permit the movement of molecules and ions, including ATP to the extracellular space and Ca^{2+} release from ER (32–34). Panx1 channels at the plasma membrane can facilitate multiple physiological and pathophysiological processes, including vascular constriction, apoptosis, tumor cell metastasis, and neuronal communication (35–38). Recently, we identified that endothelial Panx1 channel opening and ATP release promotes leukocyte recruitment (39), which plays a fundamental role in inflammation and tissue damage within ischemic stroke (40). There is increasing evidence that blocking Panx1 channels may control inflammasome activation, inflammatory cytokine release, and inflammatory cell recruitment (41–43). However, the mechanisms underlying this response have not been described. This led us to hypothesize that Panx1 signaling may be involved in the control of IL-1β production and secretion by ECs. We report in this study that EC Panx1 is a direct target of the TNF-α signaling pathway and demonstrate for the first time, to our knowledge, that Panx1 channels facilitate the transport of extracellular Ca^{2+} to promote a feed-forward effect on the synthesis of IL-1β.

Materials and Methods

All cell, media, reagent, silencing RNA (siRNA), peptide, Ab, and commercial assay information are listed in Supplemental Table I.

Primary cells and cell lines

Human umbilical vein ECs (HUVECs) and human coronary artery smooth muscle cells (SMCs) were purchased from Thermo Fisher Scientific and Cell Applications. Human Th precursor 1 (THP1) cells were a kind gift Prof. Z. Yan (University of Virginia).

Cell culture

HUVECs were grown in Medium 200 (M200) supplemented with the Low Serum Growth Kit and 20% FBS. For experiments involving TNF-α treatments, cells were incubated in M200 with Low Serum Growth Kit and 0.1% FBS (0.1%-M200) for 24 h. Human coronary artery SMCs (Thermo Fisher Scientific) were grown in Medium 231 supplemented with the Smooth Muscle Growth Supplement (Thermo Fisher Scientific) and 20% FBS. For experiments involving TNF-α treatments, cells were grown in Medium 231 containing 2% FBS. Both HUVEC and SMCs were used within 16 population doublings to maintain the primary phenotype. THP1 monocytes were grown in RPMI 1640 media supplemented with 10% FBS, 1% penicillin–streptomycin, and 1% glutamine. All cells used are certified as mycoplasma free at the start of experiments.

Cell transfection

EC were plated for expression (six-well plates) or ATP assays (24-well plates) until they were 70–80% confluent. Media was removed and replaced with 0.1%-M200 for 30 min prior to transfection. siRNAs targeting the human PANX1 gene (siPanx1; Life Technologies), or control siRNAs (siControl; Life Technologies) were transfected into ECs using Lipofectamine 3000. Media was changed after 24 h, and cells were allowed to recover for 24 h prior to treatment. siRNA knockdown for Panx1 was maximal at between 48 and 72 h and was confirmed by immunoblot and quantitative RT-PCR (qRT-PCR).

Cell treatments

Prior to treatments, media were removed from cells and replaced with 0.1% -M200 for 24 h. Media were then replaced with 0.1%-M200 containing 2.5 ng/ml TNF-α for up to 24 h (as denoted per experiment). Where TNF-α dose responses were measured, the respective concentrations are denoted in the text and figures. Inhibition of ATP (apyrase, 1 or 10 U/ml) and P2 activation [suramin, 100 μM (44)] and A438079 hydrochloride [10 μM (45–47)] were performed by 30-min preincubation prior to addition of TNF-α for a further 24 h. Inhibition of protein synthesis was performed by preincubation with 25 μg/ml cycloheximide. Inhibitors of the IKK pathway, SC514 [100 μM (48)] and QNZ/EVP4593 [10 μM (49)], and MAPK inhibitor SB203580 [10 μM (50)] were sourced from Selleck Chemicals. All kinase inhibitors were preincubated with cells for 3 h prior to treatment with TNF-α for a further 24 h. Panx1 channels were inhibited using the Panx1-specific inhibitor peptide pannexin intracellular loop 2 peptide (PxIL2P) [20 μM (51, 52)]. All inhibitors and peptide treatments were maintained in solutions throughout the experimental time course at the indicated concentrations.

RNA extraction, real-time quantitative RT-PCR, and RNA-sequencing

Following treatments, media were removed, cells were washed once in PBS, then 1 ml of TRIzol was added prior to harvesting by scraping. RNA was isolated using an RNA Isolation Kit (Bio-Rad Laboratories) as per manufacturer protocol, and cDNA synthesis was performed using a First-Strand Synthesis System (Thermo Fisher Scientific). Multiplex TaqMan reactions were performed using 20 ng of cDNA, TaqMan primers (Thermo Fisher Scientific), and TaqMan Gene Expression Master Mix (Thermo Fisher Scientific). The internal control gene GAPDH was used for normalization and calculation of the δ cycle threshold (CT) values. All data are represented as δ-δ CT (2^-ΔΔCT) to define fold change from control values. For RNA sequencing (RNA-seq), total RNA was isolated using an RNeasy Kit (QIAGEN) with an RNA-Free DNase step, and quantity was assessed on an Agilent 2100 Bioanalyzer. For experiments, three technical replicates (HUVEC, no treatment, and HUVEC plus TNF-α, 2.5 ng/ml 24 h) were sequenced with ribo-depletion protocols. After sequencing, 50-M reads were sampled from each replicate library, and results were analyzed by Glasgow Polyomics. Data from RNA-seq is available through the European Molecular Biology Laboratory–European Bioinformatics

Downloaded from http://www.jimmunol.org/ at Cochin Univ Biblio I894 on April 21, 2020

Institute ArrayExpress (https://www.ebi.ac.uk/arrayexpress/) under accession number E-MTAB-8299.

Immunoblotting and membrane protein biotinylation

Following treatments, all cells were harvested in cold lysis containing PBS (pH 7.4) containing NaCl (125 mM), EDTA (5 mM), sodium deoxycholate (1%), Triton X-100 (0.5%), sodium orthovanadate (500 μM), 4-(2-aminoethyl)benzenesulfonyl fluoride hydrochloride (10 μM), and Protease and Phosphatase Inhibitor Cocktail (1:100; Sigma-Aldrich). All isolations were performed at 4˚C, samples were Dounce-homogenized 30 times on ice, were incubated with rotation for 30 min at 4˚C, and were centrifuged at 13,000 × *g* for 5 min. Cleared lysates were used for immunoblot analysis. Proteins samples were quantified by BCA assay prior to loading, and equal loading confirmed using β-tubulin and total protein assays. Membranes were developed using LI-COR Biosciences secondary Abs, including anti-rabbit 700/800 and anti-mouse 700/800, and imaged on a LI-COR Odyssey scanner. Expression analysis was performed using Image Studio (LI-COR Biosciences). Values were normalized to β-tubulin, and changes were calculated as a fold change compared with nontreated controls. Linear ranges for the Abs used are shown in Supplemental Fig. 1, and Ab information is listed in Supplemental Table I.

Cytokine array

A Human Cytokine Array Kit (R&D Systems) were used as per manufacturers protocols, using 1 ml of cleared culture media. Media from three separate experiments under the same conditions were combined per reaction. Cytokine array membranes were developed using anti-streptavidin 800 on a LI-COR Odyssey scanner. Expression analysis was performed using Image Studio (LI-COR Biosciences). Values were normalized to the control spots on each blot, and comparisons were made to nontreated controls and expressed as a fold change from TNF-α control.

Luciferase assay for total ATP release

ATP assays were performed as we have previously described (39). Briefly, cultured ECs were seeded in 24-well plates and grown to 70–80% confluency. Media was replaced with 0.1%-M200 media containing TNF-α (2.5 ng/ml) for 24 h. On the day of the experiment, cells were rinsed, then incubated in 300 μl of fresh 0.1%-M200 media for 30 min at 37˚C, then incubated with the ectonucleotidase inhibitor ARL 67156 (300 μM; Tocris Bioscience) for 30 min at 37˚C. TNF-α was maintained at indicated concentrations throughout all incubations and washes. Cells were then stimulated with recombinant human TNF-α (10 ng/ml) for 5 min to produce maximal Panx1 channel activation, as previously described (39). Following stimulation, 200 μl of the cell supernatants were collected, placed into prechilled tubes, centrifuged at 10,000 × *g* for 5 min, and 50 μl of each sample was transferred to a white, opaque 96-well plate. ATP was measured using ATP bioluminescence assay reagents, including CellTitre Glo 2.0 (Promega) or ATP Bioluminescence HSII Kit (Roche). Using a luminometer (FLUOStar Omega), 50 μl of luciferin:luciferase reagent (ATP Bioluminescence Assay Kit HSII; Roche) was injected into each well, and luminescence was recorded following a 5-s orbital mix and sample measurement at 7 s. For CellTitre Glo 2.0, the reagent was mixed 50:50 with cleared HUVEC media, and the luciferase signal was measured within 10 min. The ATP concentration in each sample was calculated from an ATP standard curve. Data are presented either as calculated concentration or as a percentage change in ATP release from baseline (unstimulated cells) and expressed as mean ± SEM (n = 5 independent experiments with triplicate measurements).

Cell membrane luciferase reporter of ATP release

HUVEC cells (1×10^6) were trypsinized, pelleted at 700 rpm, then mixed with primary EC nucleofection reagents (Lonza) and 20 μg of plasma membrane luciferase (pmeLUC) plasmid (53) prior to nucleofection on a nucleofector 2b (Lonza). Following transfection, cells were resuspended in M200 with 20% FBS and plated in fibronectin-coated, white-walled 96-well plates. After 24 h, cells were treated with TNF-α (2.5 ng/ml) as indicated in 0.1%-M200 for a further 24 h. Cells were washed, and media were replaced with media containing TNF-α (as denoted per experiment). For standard curves, nontreated pmeLUC-transfected HUVECs were incubated with ATPγS (as denoted per experiment). D-Luciferin was injected into each well individually, and luminescence was recorded at 7 s, following a 5-s orbital mix (FLUOstar Omega plate reader).

Flow cytometric analysis of $[Ca^{2+}]_i$

HUVECs were seeded on fibronectin-coated plates and grown to 90% confluence. Cells treated with siRNA, the Panx1 inhibitor peptide PxIL2P (20 μM), and TNF-α (as denoted per experiment), were incubated with Fluo-4 acetoxymethyl ester (AM) [2 μM (54)] plus 0.1% Pluronic for 30 min, then cells were harvested by trypsinization, centrifuged, and resuspended in 0.1% media containing either no treatment, TNF-α (2.5 ng/ml), or PxIL2P with TNF-α (2.5 ng/ml) and stored on ice for analysis by flow cytometry (BD FACSCanto II). Gates for Fluo-4–positive cells were defined, and absolute fluorescence intensity was calculated. TNF-α treatments and inhibitors were maintained in solutions throughout the experiments as indicated. Concentrations for maximal Fluo-4 signal were calibrated for flow cytometry, and consistent experimental conditions were maintained throughout. The concentration of 2 μM Fluo-4 loading for FACS was determined as the optimum condition that permitted measurable signal differences for Fluo-4 signal without saturation, compared with non–Fluo-4 loaded cells.

Flow cytometric analysis of monocyte adhesion

HUVECs were seeded on fibronectin-coated plates and grown to 70% confluence. Cells were washed twice in warmed PBS, and media were changed for 0.1%-M200 for 24 h. Media were changed for 0.1%-M200 with TNF-α (2.5 ng/ml) for 24 h. At the same time, human THP1 monocytes were loaded with calcein AM (0.1 μM; Sigma-Aldrich) in RPMI 1640 for 30 min. THP1 cells were then centrifuged and washed twice in PBS prior to being resuspended in 10% RPMI 1640 media for 24 h. After 24 h, TNF-α was removed from HUVECs by washing once in 0.1%-M200, and cells were incubated in fresh 0.1%-M200 for 30 min. During this time, calcein-loaded THP1 cells were counted and resuspended to a concentration of 5×10^5 cells/ml in 0.1%-M200. THP1 cells (100 μl, 5×10^4) were added to each well for 4 h at 37˚C. After 4 h, the wells were washed gently two times with PBS to remove nonadherent cells. All remaining cells were then trypsinized and resuspended in 0.1%-M200 media and stored on ice for analysis by flow cytometry (BD FACSCanto II). Gates for calcein-stained THP1 and nonstained ECs were defined, and the percentage of THP1 monocytes was calculated from the total cells (EC and THP1 cells).

Confocal imaging of $[Ca^{2+}]_i$

HUVECs were seeded on fibronectin-coated plates and treated with TNF-α as indicated. TNF-α treatment was maintained in all washes and incubations. Cells were washed using HEPES physiological salt solution (HPSS) containing HEPES 10 mM, sodium chloride 134 mM, potassium chloride 6 mM, magnesium chloride hexahydrate 2.15 mM, calcium chloride 2mM, and dextrose 7 mM, then incubated in HPSS containing Fluo-4 AM [5 μM (55)] and 0.2% Pluronic for 30 min at room temperature. Concentrations for maximal Fluo-4 signal were calibrated for confocal imaging, and consistent experimental conditions were maintained throughout. Cells were then washed in HPSS and maintained in HPSS containing the cyclopiazonic acid (20 μM), to eliminate interfering inositol 1,4,5-trisphosphate receptor–mediated Ca2+ signals (56, 57), and TNF-α as indicated for 10 min prior to imaging. HUVEC Fluo-4 fluorescence was imaged on an inverted confocal microscope (FV3000; Olympus) using a 40× lens under 2× zoom. Experiments were performed in triplicate, and three regions containing ∼10–15 cells per field of view per plate were imaged at 1-s intervals for 2 min. Average and maximum fluorescence measurements within the cytoplasmic regions of each cell were averaged for each region, then averaged per experiment (n = 4). To determine maximum concentrations for Fluo-4 loading, cells were incubated with concentrations ranging between 2 and 10 μM, and signals were measured. The optimum condition of 5 μM was determined as the signal that did not produce fluorescence signal saturation during Ca^{2+} wave formation in TNF-α–treated cells while maintaining measurable signal within the untreated cells.

IL-1β ELISA

HUVEC cells were treated with siPanx1 or siControl or in the presence of the PxIL2P (20 μM), then treated with TNF-α (2.5 ng/ml, 24 h, as indicated). Following incubation, media were collected and spin concentrated 5 times in a centrifugal filter (Amicon Ultracel 3K). Concentrated samples were analyzed for IL-1β expression by ELISA (IL-1 beta SimpleStep ELISA Kit; Abcam) as per the manufacturer's instructions, and concentrations were calculated against standard controls for IL-1β. Experiments were performed in triplicate.

Quantification and statistical analysis

A one-way or two-way ANOVA followed by a Tukey or Dunnett posttest was used for comparisons between three groups, and a t test was used for comparisons of two treatment groups. A minimum of n = 3 was used for all statistical analysis. In all analysis, a p value < 0.05 is significant as denoted as $*p < 0.05$, $***p < 0.01$, $***p < 0.001$, and $****p < 0.0001$.

Downloaded from http://www.jimmunol.org/ at Cochin Univ Biblio I894 on April 21, 2020

Results

TNF-α induces Panx1 expression and membrane targeting of Panx1 channels in ECs

In HUVECs, we initially demonstrate that prolonged exposure to TNF-α (2.5 ng/ml) for 5 and 24 h leads to an increase in the transcription of Panx1, measured by qRT-PCR (Fig. 1A). Increases in Panx1 mRNA levels correlate with significant increases in protein expression of Panx1 at 5 h measured by immunoblotting (Fig. 1B). The multiple banding pattern for the Panx1 protein observed in immunoblots represents differential Panx1-glycosylation (Panx1-Gly) isoforms, referred to as Panx1-Gly0, -Gly1, and -Gly2 (58–60). Interestingly, we observed that at 5 h TNF-α treatments primarily increase only Panx1-Gly0 and Panx1-Gly1 isoforms, which were ablated by cotreatment with the protein synthesis inhibitor cycloheximide (CHX, Fig. 1B, Supplemental Fig. 2A), suggesting that these isoforms represent newly synthesized Panx1 protein. To determine the specificity of TNF-α to Panx1 expression, we investigated the Cx43 gap junction protein in HUVECs, which did not increase following TNF-α stimulation and was inhibited following CHX treatments (Fig. 1B). Following 24-h TNF-α treatment, we identified significant upregulation of the Panx1-Gly2 isoform (Supplemental Fig. 2B). Increasing the concentration of TNF-α treatments did not enhance Panx1 expression from 2.5 ng/ml at either 5 h or 24 h and did not alter expression of Cx43 (Supplemental Fig. 2A–C). In addition, Panx1-Gly2 isoforms were not reduced by CHX (Fig. 1B), suggesting that these represent a more stable isoform of Panx1. To investigate this, HUVECs were treated with TNF-α for 24 h, washed in fresh media without TNF-α, and cultured for a further 8 d. Analysis by immunoblot demonstrates that, whereas the Panx1-Gly0/1 isoforms are lost within 24 h of removal of TNF-α, the Panx1-Gly2 isoforms remain significantly increased from control for 24 h after removal of TNF-α and remain elevated for a further 5 d (Fig. 1C). This demonstrates a stable, mature form of Panx1 that has a significant residence time at the plasma membrane, making it more stable than connexin proteins.

Previous studies have suggested that Panx1-Gly2 isoforms represent the mature Panx1 channels within the plasma membrane (60). We therefore used a membrane protein biotinylation pull-down approach to isolate plasma membrane proteins and identified that Panx1-Gly2 isoforms are primarily localized within the plasma membrane 24 h after TNF-α treatment (Fig. 1D). We further demonstrate that Panx1 expression by cultured human vascular SMC is unaltered by TNF-α treatment (Supplemental Fig. 2D). Previous studies have found TNF-α to reduce cell viability (61). However, 24-h TNF-α treatments ranging from 2.5 to 100 ng/ml did not alter HUVEC viability as measured by intracellular ATP levels, caspase-3 cleavage, or by cell morphology (Supplemental Fig. 2E–G).

TNF-α signaling is associated with activation of NF-κB–mediated gene regulation. Whole transcriptome RNA-seq experiments confirmed that TNF-α treatment of HUVECs significantly upregulated NF-κB genes NFKBIA, NFKBIE, NFKB1, NFKB2, and NFKB1B (Fig. 1E). To define a role for NF-κB–activated pathways in TNF-α–induced increases in Panx1 expression, HUVECs were pretreated with NF-κB inhibitors SC514 and QNZ. Both SC514 and QNZ significantly ablated TNF-α–induced increases in Panx1 expression at 24 h (Fig. 1F, 1G). RNA-seq results demonstrate that TNF-α (2.5 ng/ml) does not alter MAPK transcription, and MAPK inhibition failed to reduce TNF-α–associated Panx1 upregulation (Supplemental Fig. 2H, 2I). This suggests that TNF-α specifically stimulates a NF-κB–mediated upregulation of Panx1 proteins, leading to plasma membrane localization of Panx1 channels in ECs.

Increased Panx1 membrane targeting is associated with the transcription and release of specific proinflammatory cytokines

Panx1 has been associated but not directly implicated in the release of molecules associated with inflammation (39, 62, 63). To investigate whether the increased Panx1 at the plasma membrane is directly associated with cytokine production and release, we first used genetic inhibition of Panx1. Panx1 siRNA reduced the basal expression of Panx1 in HUVECs and inhibited increases in Panx1 in response to TNF-α (Fig. 2A, 2B). Cytokine arrays used to assay the media from HUVEC cells showed that TNF-α treatment altered the expression of a number of cytokines (Supplemental Fig. 3A). We selected key proinflammatory cytokines associated with atherosclerosis, such as IL-1β and CXCL10, IL-8, and MCP-1, which were found to be increased in response to TNF-α treatment in HUVECs, unlike MIF and Basigin, which were not markedly increased by TNF-α (Fig. 2C). We confirmed that TNF-α increases IL-1β protein expression in HUVECs (Supplemental Fig. 3B) and that siRNA knockdown of Panx1 was associated with a reduction in the release of IL-1β from HUVECs (Fig. 2D). Notably, Panx1 siRNA–treated cells displayed a significantly reduced transcription of IL-1β and CXCL10 but showed no differences in IL-8 and CCL2 (Fig. 2E, 2F). Panx1 siRNA and TNF-α treatments also had no effect on MIF or CD147 (Fig. 2G). These data suggest that Panx1 critically regulates the control of specific inflammatory cytokines, including IL-1β and CXCL10. Although multiple other cytokines and chemokines have been found to be increased in atherosclerosis, clinical trials targeting these pathways by treatments, including low-dose methotrexate have not proven to be effective in reducing the burden of disease in patients (18). Based on this, we focused on mechanisms controlling IL-1β, because directly targeting IL-1β is linked with a reduction in patient risk (16). Critically, understanding the molecular mechanisms controlling IL-1β expression may provide avenues for future therapeutic intervention (2, 3, 64–66).

Purinergic signaling is not a key regulator of TNF-α–induced IL-1β in ECs

Based on the known role for Panx1 and ATP release, which has been linked with IL-1β regulation, we investigated ATP release from HUVECs following treatment with TNF-α and the corresponding effects of ATP on IL-1β. ATP release from HUVECs was measured in media following TNF-α treatment at doses ranging from 2.5 to 100 ng/ml. All concentrations of TNF-α produced similar increases in ATP release from HUVECs (Fig. 3A), which was significantly reduced following genetic inhibition of Panx1 (Fig. 3B). Although previous studies have correlated ATP treatment with regulation of IL-1β, this has typically required ATP analogues to be applied at nonphysiological concentrations ranging from 100 μM to 5 mM (22–24). Our data demonstrate that the HUVECs release only 10–20 nM ATP once exposed to TNF-α (2.5 ng/ml) for 24 h (Fig. 3C). At these concentrations (10 nM–10 μM), the ATP analogue ATPγS failed to increase IL-1β transcription (Fig. 3D). However, we did observe a small increase in transcription of IL-1β at 100 μM ATPγS, which could be ablated by pretreating and maintaining cells with the P2X inhibitor suramin (Fig. 3E). To understand whether plasma membrane levels of ATP reached 100 μM in HUVECs following TNF-α treatment, cells were transfected with the pmeLUC plasmid (53) to produce plasma membrane expression of the luciferase enzyme. The HUVECs pmeLUC signal was detected at above 10 μM ATPγS, in keeping with previous publications (53). However, TNF-α treatment of HUVECs (2.5 ng/ml, 24 h) did not induce significant alterations in pmeLUC signal (Supplemental Fig. 4A). Further data demonstrate that promoting the degradation of released ATP using apyrase

Downloaded from http://www.jimmunol.org/ at Cochin Univ Biblio I894 on April 21, 2020

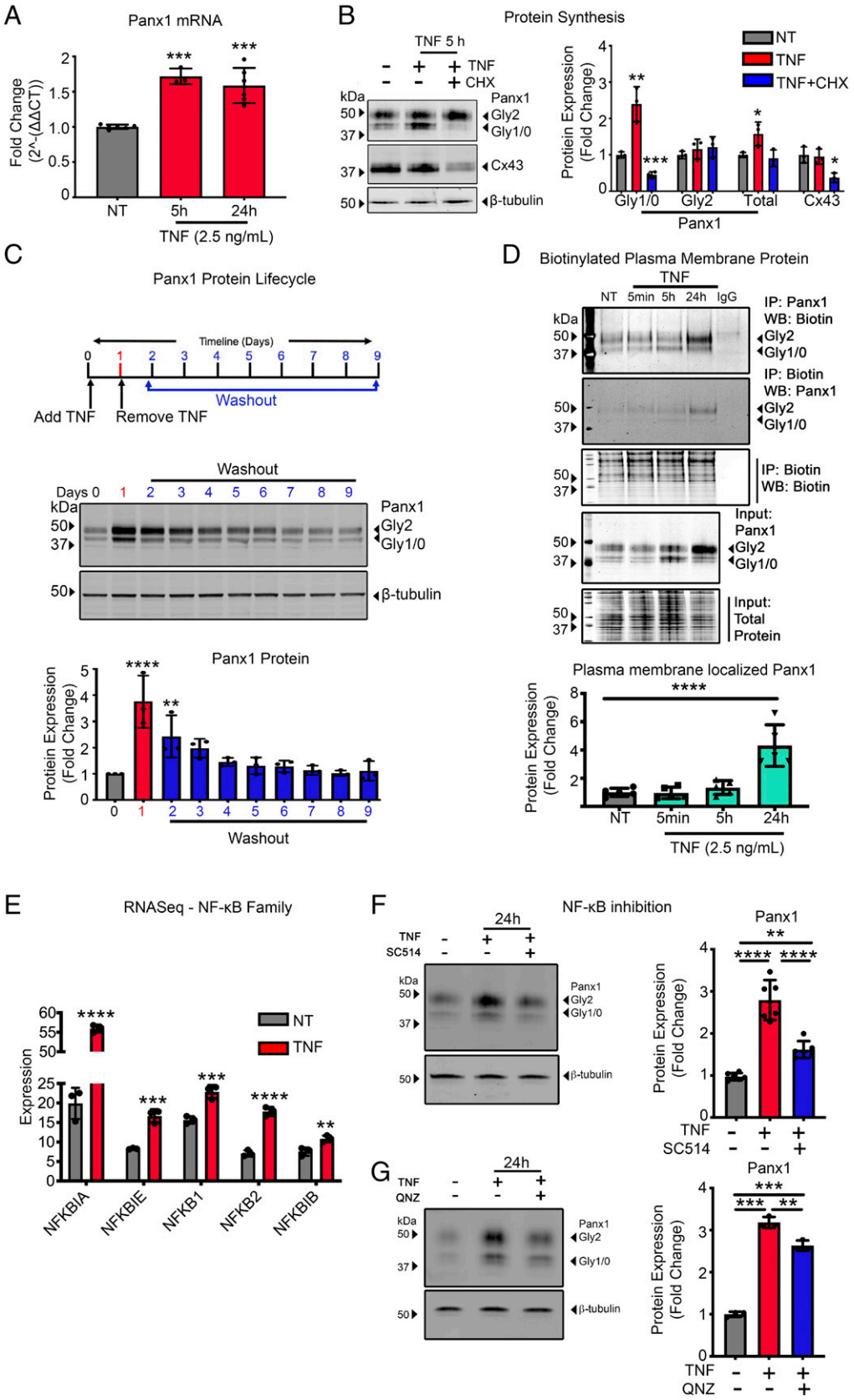

FIGURE 1. TNF-α transcriptional regulation of Panx1 through the NF-κB pathway promotes protein synthesis and plasma membrane trafficking. (**A**) TaqMan qRT-PCR of RNA extracted from HUVECs treated with TNF-α (2.5 ng/ml) for 5 and 24 h. The mean of Panx1 expression was normalized to control and calculated to 2^-ΔΔCT. For each error bar, reactions were performed in triplicates in addition to the technical triplicates. (**B**) Representative immunoblots of Panx1 and Connexin 43 (Cx43) in HUVECs pretreated with CHX for 30 min and subsequent TNF-α (2.5 ng/ml) treatment for 24 h. Quantification of Panx1 expression was normalized to β-tubulin ($n = 3$). (**C**) Upper panel, Schematic of HUVECs treatment approach to assess Panx1 protein lifecycle. Black arrowheads mark the time TNF-α was added and removed. The blue scale marks cells maintained in 0.1%-M200 (no TNF-α) collected each 24 h after TNF-α removal. Lower panel, Representative immunoblots of Panx1 and β-tubulin expression and quantification *(Figure legend continues)*

Downloaded from http://www.jimmunol.org/ at Cochin Univ Biblio I894 on April 21, 2020

(at 1 and 10 U) or inhibition of the P2 receptors using either suramin or the P2 inhibitor A438079 hydrochloride (10 μM), did not significantly alter the expression of either Panx1 or IL-1β in the presence of TNF-α (Fig. 3F, 3G, Supplemental Fig. 4B). Thus, the NF-κB–induced increase in Panx1 expression at the plasma membrane, although crucial for IL-1β cytokine production, was not regulated by an autocrine ATP release from the ECs.

TNF-α increases $[Ca^{2+}]_i$, which is regulated by the functional Panx1 channels

Increased $[Ca^{2+}]_i$ is associated with the control of IL-1β synthesis (31), and Panx1 channels have been suggested to allow the passage of Ca^{2+} from the extracellular environment into the cytosol, albeit this has never been demonstrated (33, 67). To investigate whether Panx1 plays a role in the control of $[Ca^{2+}]_i$ we used a high-throughput flow cytometric approach (54) to measure $[Ca^{2+}]_i$ in HUVECs. We found that $[Ca^{2+}]_i$ was only increased after 24-h TNF-α treatment, a time that correlates with the increases in Panx1 membrane localization (Fig. 4A). These finding were confirmed using confocal imaging of Fluo-4–labeled HUVECs, in which TNF-α induced a higher baseline Fluo-4 signal associated with increased calcium wave formation (Supplemental Fig. 5A–C). To determine whether increases in $[Ca^{2+}]_i$ were due to extracellular Ca^{2+} (e.g., through the increased number of Panx1 channels), Ca^{2+}-free Kreb–Ringer was used. This experiment demonstrated a significant decrease in EC $[Ca^{2+}]_i$ (Fig. 4B). We further demonstrated that increased $[Ca^{2+}]_i$ is directly related to IL-1β production because cells loaded with EGTA-AM in the media reduced $[Ca^{2+}]_i$, which corresponded to a loss of TNF-α–induced IL-1β transcription (Fig. 4C, 4D). To more specifically assess whether there was a role for Panx1 in regulating EC $[Ca^{2+}]_i$, we used the Panx1-specific channel blocking peptide PxIL2P to pharmacologically inhibit Panx1 channels (51, 52). Pretreatment of HUVECs with PxIL2P reduced $[Ca^{2+}]_i$, IL-1β transcription, and IL-1β release in response to 24-h TNF-α treatment (Fig. 4E–G) and release. Similar results were found using genetic inhibition of Panx1, which reduced TNF-α–associated increases in $[Ca^{2+}]_i$ (Fig. 4H) and IL-1β (Fig. 2E). In line with these observations, there was also a decrease in monocyte binding to ECs following genetic inhibition of Panx1 in ECs, with no change in THP1–Panx1 expression associated with TNF-α treatments (Supplemental Fig. 5D, 5E). Lastly, levels of $[Ca^{2+}]_i$ and IL-1β mRNA were reduced 24 h after the removal of TNF-α (Fig. 4I, 4J), which correlated with the same decrease in Panx1 expression at the plasma membrane seen in Fig. 1C. These data provide additional evidence that increased Panx1 channels in EC after TNF-α stimulation permit the passive diffusion of extracellular Ca^{2+} into the cell, possibly to regulate IL-1β production.

Because increased $[Ca^{2+}]_i$ has been reported to result in phosphorylation of the NF-κB protein p65 (p-p65), increasing its transcriptional activity (68), we aimed to assess the role of Panx1 in regulating NF-κB–p-p65. HUVEC treatment with TNF-α (24 h) leads to an increase in p-p65, which was significantly decreased following genetic (siRNA of Panx1) or pharmacological (PxIL2P) inhibition of Panx1 (Fig. 4J, 4K). Taken together, these data suggest that Panx1 channels in the plasma membrane act as a conduit for the movement of Ca^{2+} into the cytosol, leading to activation of NF-κB signaling, which acts as a feed-forward mechanism to promote the production and release of IL-1β.

Discussion

ATP release through Panx1 channels has been shown to be a strong signal for the recruitment of inflammatory cells in response to apoptosis (35) and activation of the NLRP3 inflammasome (42, 43, 69). However, the precise Panx1-mediated mechanisms controlling inflammation have never been fully elucidated. In this study, we demonstrate that EC Panx1 is a direct target of the TNF-α signaling pathway, promoting plasma membrane localization of the channel, which facilitates the entry of extracellular Ca^{2+} into the cytosol. Importantly, we show that increases in $[Ca^{2+}]_i$, resulting from enhanced Panx1 channel activity are directly associated with upregulated transcription and release of proinflammatory cytokines, including IL-1β.

One of the primary findings in this study is the identification of a novel mechanism for the transcriptional regulation of Panx1. We observed that EC Panx1 is acutely sensitive to TNF-α stimulation, with maximal increases found in the low nanogram/milliliter range. Our data suggest that this is not a ubiquitous pathway, as increases in Panx1 expression were not found in TNF-α–treated SMCs or monocytes. Both SMCs and monocytes express TNF-α receptors and form inflammatory responses to TNF-α stimulation (70–72). It is possible that cell-specific variances in gene or protein regulation in these cells may be due to differential regulation of receptor activation (72) or downstream pathways [e.g., SMC ubiquitin-specific protease 20 [USP20]–deubiquitinase activity, which reduces NF-κB in SMC (71)]. There are few studies that have investigated the transcriptional control of Panx1, and there are currently limited data on pathophysiological mechanisms controlling Panx1 expression (73). Jiang et al. (74) reported increases in expression of Panx1 in mouse models of inducible stroke, which are associated with increased TNF-α–induced inflammation and tissue injury (75–78). In silico analysis has highlighted a number of transcriptional start sites within the rat Panx1 sequence, with binding sites for several transcription factors, including CREB and ETV4 as well as factors downstream from IL-6 that have been identified (79). Our RNA-seq data highlighted that TNF-α upregulates all NF-κB genes in HUVECs. TNF-α–induced Panx1 transcription was lost when HUVECs were pretreated with inhibitors shown to block NF-κB–IKKB activity and TNF-α production (48, 80, 81). Our data strongly suggest that NF-κB pathways regulate EC Panx1 transcription.

We also found that increases in Panx1 transcription are followed by protein translation within 5 hours that was lost when cells were treated with the protein synthesis inhibitor CHX. The newly synthesized Panx1 proteins then translocate to the plasma membrane within 24 hours. Our surface biotinylation experiments highlight that the Panx1 isoform at the plasma membrane is primarily the complex glycoprotein isoform (Panx1-Gly2). This is in keeping with previous studies that suggest that the Panx1-Gly2 is

of Panx1 expression under these treatment conditions ($n = 3$). (**D**) Representative immunoblots of HUVECs treated with TNF-α (2.5 ng/ml) for a time course of 5 min, 5 and 24 h, and subsequent immunoprecipitation of cell surface–biotinylated membrane proteins. Plasma membrane–localized Panx1 expression was normalized to biotin-labeled total protein ($n = 5$). (**E**) RNA-seq performed on HUVECs treated with TNF-α (2.5 ng/ml) for 24 h. The expression of five genes in NF-κB family are shown, with each bar representing mean ± SD for triplicates ($n = 3$). (**F** and **G**) Representative immunoblots of TNF-α–induced (2.5 ng/ml) HUVECs in presence or absence of inhibitors, including inhibitor of NF-κB kinase-2 (IKK2) 100 μM SC514 ($n = 5$) or NF-κB inhibitor 10 μM QNZ ($n = 3$) for 24 h. Statistical analyses were performed by one-way or two-way ANOVA with either Dunnett or Tukey multiple comparison test. $^*p < 0.05$, $^{**}p < 0.01$, $^{***}p < 0.001$, $^{****}p < 0.001$. TNF, TNF-α.

Downloaded from http://www.jimmunol.org/ at Cochin Univ Biblio I894 on April 21, 2020

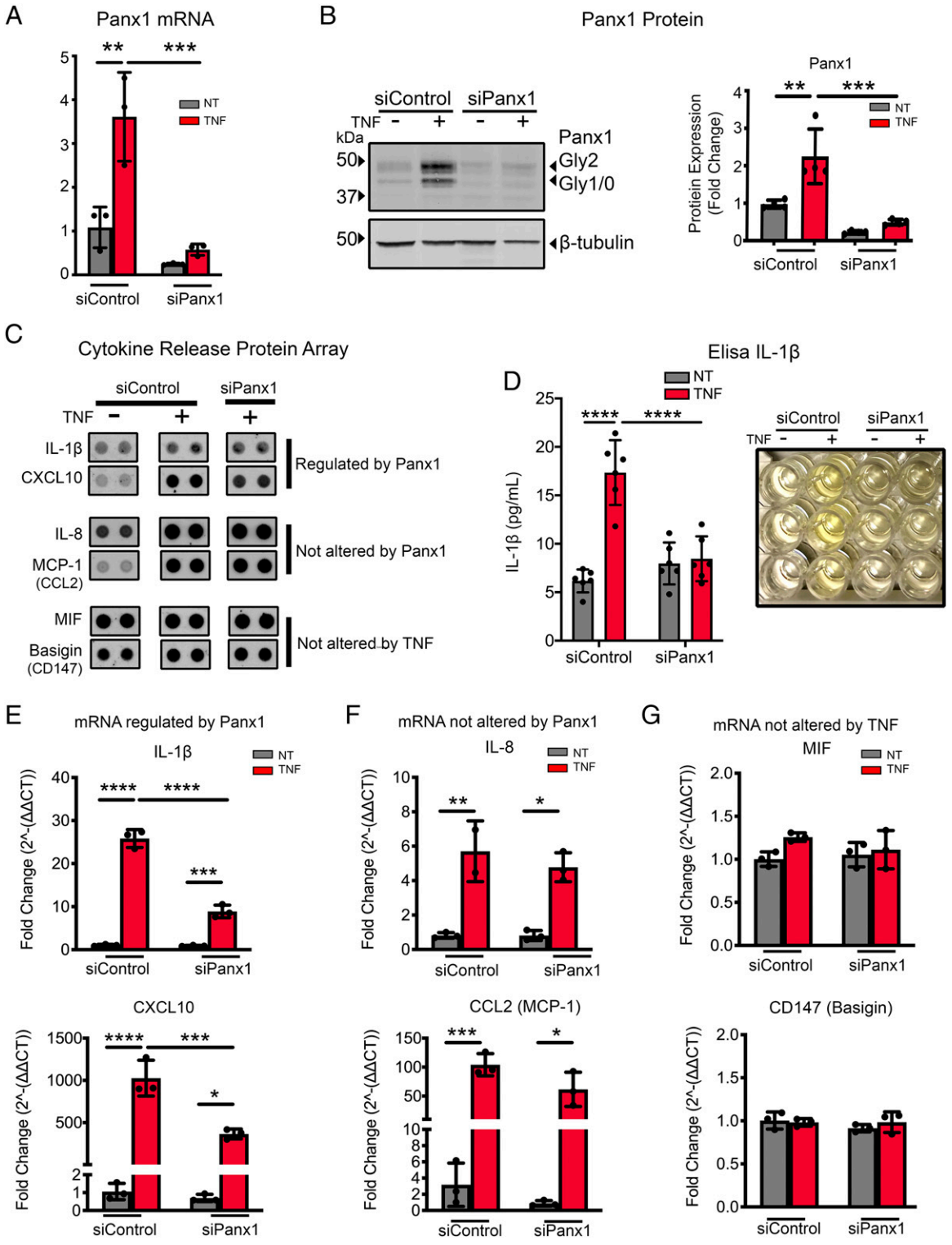

FIGURE 2. Panx1 controls transcription of selective inflammatory cytokines. (**A**) qRT-PCR analysis of Panx1 in HUVECs transfected with siControl or siRNA Panx1 for 48 h followed with 24-h TNF-α (2.5 ng/ml) treatment. Each reaction was performed in triplicates in addition to the technical triplicates ($n = 3$). (**B**) Representative immunoblot of Panx1 in HUVECs transfected with siControl or siRNA Panx1 for 48 h followed by 24-h TNF-α (2.5 ng/ml) treatment. Panx1 expression was normalized to β-tubulin and expressed as fold change ($n = 4$). (**C**) Cell media collected from HUVECs transfected with siControl or siRNA Panx1 for 48 h followed with 24-h TNF-α (2.5 ng/ml) treatment were incubated with a human cytokine array ($n = 2$). Representative cytokine spot duplicates for selected groups (IL-1β, CXCL10, IL-8, MCP-1, MIF, and Basigin) are shown. (**D**) ELISA of IL-1β release in media from HUVECs transfected with siControl or siRNA Panx1 for 48 h followed with 24-h TNF-α treatment (2.5 ng/ml). Each measurement was performed ($n = 6$) times; a representative image is shown for treatment groups. qRT-PCR analysis of the expression of IL-1β and CXCL10 (**E**), IL-8 and CCL2 (**F**), and MIF and CD147 (**G**) in HUVECs transfected with siControl or siRNA Panx1 for 48 h followed with 24-h TNF-α treatment (2.5 ng/ml). Cytokines were normalized to control and calculated to 2^-ΔΔCT, then expressed as fold change. Each group was performed in triplicates in addition to the technical triplicates ($n = 3$). Statistical analyses were performed by one-way or two-way ANOVA with either Dunnett or Tukey multiple comparison test. $*p < 0.05$, $**p < 0.01$, $***p < 0.001$, $****p < 0.001$. TNF, TNF-α.

Downloaded from http://www.jimmunol.org/ at Cochin Univ Biblio I894 on April 21, 2020

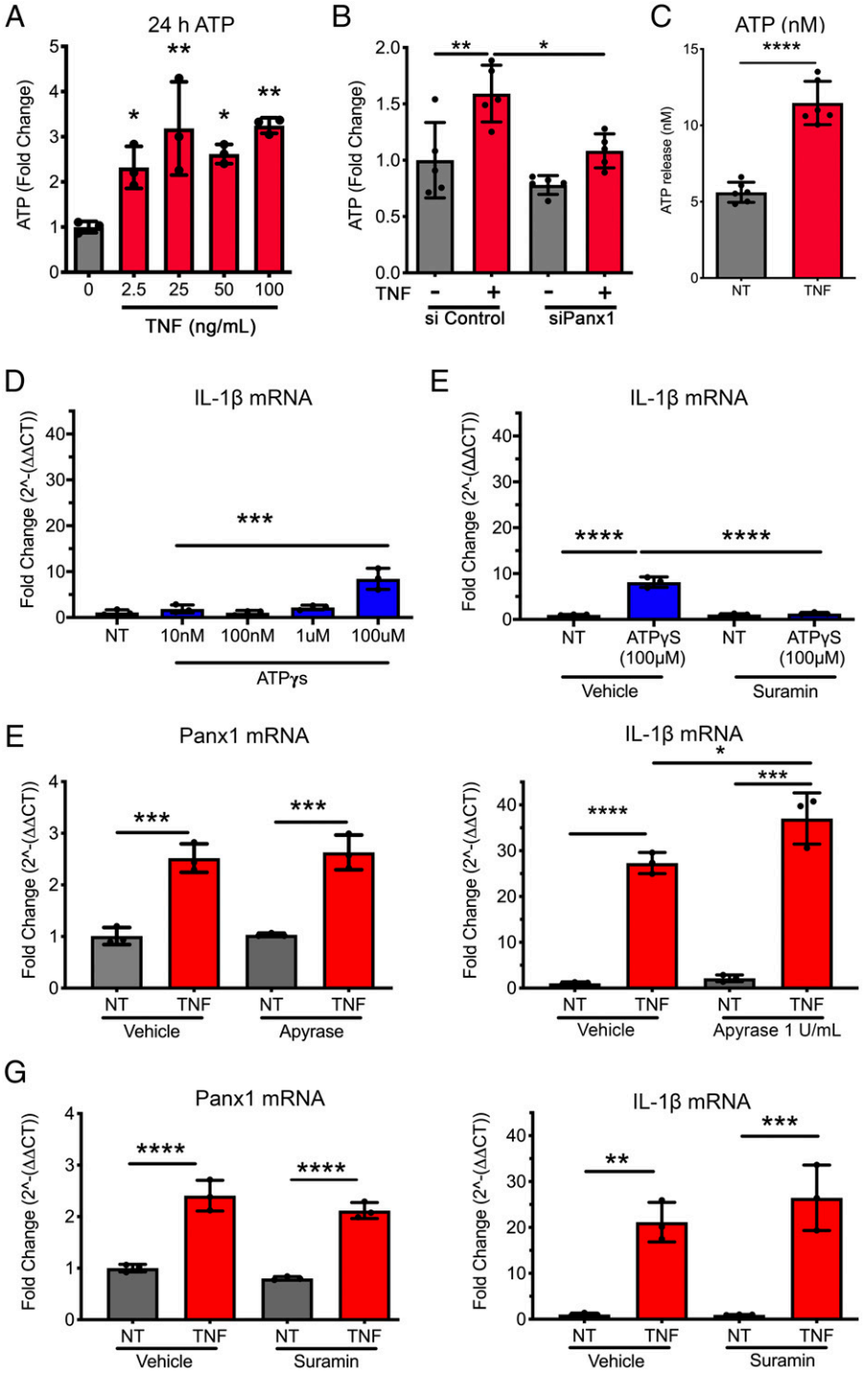

FIGURE 3. ATP release through Panx1 channel opening is not associated with IL-1β regulation. (**A**) ATP release measured and quantified as fold change from control (0 ng/ml TNF-α) to HUVECs pretreated with TNF-α (0, 2.5, 25, 50, 100 ng/ml) for 24 h ($n = 3$). (**B**) ATP release measured and quantified as fold change from control (siControl or siPanx1), with 24 h incubation of TNF-α (2.5 ng/ml) ($n = 5$). (**C**) Calculated mean extracellular ATP concentration from 24-h TNF-α pretreatment HUVECs in response to TNF-α (10 ng/ml) for 5 min ($n = 6$). (**D**) qRT-PCR analysis of IL-1β expression in HUVECs applied to a dose response for exogenous ATPγS (10, 100 nM, 1, and 100 μM) to assess the potential effect on IL-1β upregulation ($n = 3$). Data were normalized to control and calculated to 2^-ΔΔCT, then expressed as fold change. Each group was performed in triplicates in addition to the technical triplicates ($n = 3$). (**E**) qRT-PCR analysis of IL-1β in HUVECs treated with ATPγS (100 μM) in the presence of suramin to (100 μM) to block P2X receptors ($n = 3$). Data were normalized to control and calculated to 2^-ΔΔCT, then expressed as fold change. Each group was performed in triplicates in addition to the technical triplicates ($n = 3$). (**F**) qRT-PCR analysis of Panx1 and IL-1β in HUVECs pretreated with apyrase (1 U/ml) to degrade extracellular ATP, then with TNF-α (2.5 ng/ml) plus apyrase (1 U/ml) for 24 h ($n = 3$). Data were normalized to control and calculated to 2^-ΔΔCT, then expressed as fold change. Each group was performed in triplicates in addition to the technical triplicates ($n = 3$). (**G**) qRT-PCR analysis of Panx1 and IL-1β in HUVECs pretreated with suramin (100 μM), to block P2X receptor activity, then with TNF-α (2.5 ng/ml) plus suramin (100 μM) for 24 h ($n = 3$). Data were normalized to control and calculated to 2^-ΔΔCT, then expressed as fold change. Each group was performed in triplicates in addition to the technical triplicates ($n = 3$). Statistical analyses were performed by one-way or two-way ANOVA with either Dunnett or Tukey multiple comparison test. $^*p < 0.05$, $^{**}p < 0.01$, $^{***}p < 0.001$, $^{****}p < 0.001$. TNF, TNF-α.

the predominant posttranslationally modified form of Panx1 in the plasma membrane that forms hexameric membrane channels (58, 60). Pannexins are close family members of the connexin protein family, which have a protein half-life of between 1 and 4 hours (82, 83). An interesting observation in our study was that, once at the plasma membrane, the Panx1-Gly2 isoform is highly stable, unlike Cx43, and may persist for several days after the removal of TNF-α. This represents significantly longer protein stability than previously reported in experimental models by Boassa et al. (60, 84) and may highlight different protein recycling pathways between cell types. Despite having an extended residence time at the plasma membrane, our data also reveal that the Panx1 channel activity may be dependent on continued stimulation by TNF-α for channel opening (as described in Ref. 85) because $[Ca^{2+}]_i$ were reduced to baseline within 24 hours of the removal of TNF-α. Thus, Panx1 functions in ECs are regulated by TNF-α through multiple mechanisms, including synthesis, translation, trafficking, and channel opening via phosphorylation.

Recent clinical trials have demonstrated that inflammation plays a key role in atherosclerotic disease development and that targeting specific cytokines may provide therapeutic benefits in high-risk patients (3, 14, 16, 18, 64, 86). In particular, the Canakinumab Anti-inflammatory Thrombosis Outcome Study trial demonstrated that canakinumab, an anti–IL-1β therapeutic, reduces circulating levels of IL-1β in patients and decreases major adverse coronary events. Canakinumab treatments reduce IL-1β expression but also

Downloaded from http://www.jimmunol.org/ at Cochin Univ Biblio I894 on April 21, 2020

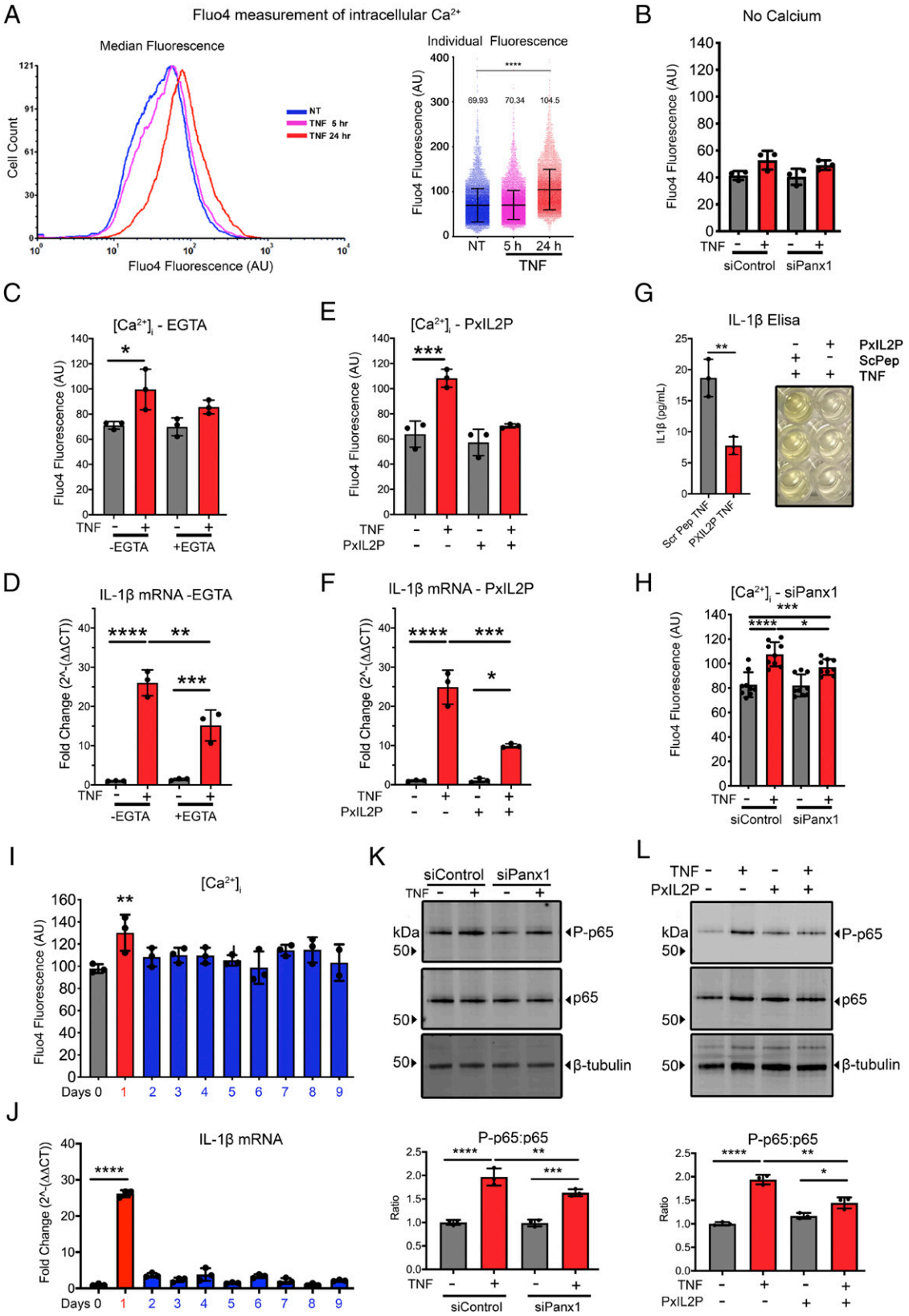

FIGURE 4. Panx1 facilitates increased $[Ca^{2+}]_i$ associated with inflammatory regulation. (**A**) Representative flow cytometry $[Ca^{2+}]_i$ traces from HUVECs treated with TNF-α (2.5 ng/ml) for 24 h (red) compared with control (blue) and 5-h treatment (magenta). Graphs of individual cell Fluo-4 fluorescence of $[Ca^{2+}]_i$ compared with control as indicated ($n = 3$). (**B**) Flow cytometric measurement of median $[Ca^{2+}]_i$ in HUVECs transfected with siControl or siRNA Panx1 for 48 h followed with 24-h TNF-α treatment (2.5 ng/ml) measured in calcium-free Krebs solution ($n = 3$). (**C**) Flow cytometric measurement of median $[Ca^{2+}]_i$ in HUVECs treated with TNF-α (2.5 ng/ml) for 24 h in presence of a chelator of calcium EGTA-AM ($n = 3$). (**D**) qRT-PCR analysis of IL-1β expression in HUVECs treated with TNF-α (2.5 ng/ml) for 24 h in the presence of a chelator of calcium EGTA-AM ($n = 3$). Data were normalized to control and calculated to 2^-ΔΔCT, then expressed as fold change. Each group was performed in triplicates in addition to the technical triplicates ($n = 3$). (**E**) Flow cytometric measurement of median $[Ca^{2+}]_i$ in HUVECs pretreated with PxIL2P peptide (20 μM) followed by TNF-α (2.5 ng/ml) *(Figure legend continues)*

Downloaded from http://www.jimmunol.org/ at Cochin Univ Biblio I894 on April 21, 2020

reduce expression of biomarkers, including IL-6 and C-reactive protein (16). However, targeting pathways associated with IL-6 expression using low-dose methotrexate did not result in significant patient benefits (18, 87, 88). This has led to the suggestion that atherosclerosis may be under the control of IL-1β and that targeting pathways controlling or controlled by IL-1β may have therapeutic benefit (2, 3, 64–66). In this study, we show that TNF-α treatment of HUVEC cells leads to release of cytokines, including IL-1β, which was significantly reduced when Panx1 expression was knocked down via siRNA. Approaches using genetic (siRNA of Panx1) or pharmacological (PxIL2P) inhibition further identified that Panx1 expression and signaling can regulate IL-1β synthesis and release. These data suggest that Panx1 may be involved in multiple aspects of the synthesis and release of IL-1β in ECs.

Our data provide further evidence that the expression of other inflammatory chemokines, such as CXCL10, is controlled in a Panx1-specific manner. CXCL10 has been proposed to be an important inflammatory marker in atherosclerosis (89, 90), leading to the formation of vulnerable plaques in humans and mice (91, 92). Strategies to lower CXCL10 expression can lead to reduced plaque formation and increased plaque stability (91). As previously described, it is possible that these increases correlate with IL-1β signaling pathways (2, 3, 64–66). However, the mechanisms through which Panx1 regulates these cytokines and chemokines remain to be fully elucidated.

The primary focus for signaling via Panx1 channels has been the release of ATP following channel opening (35, 39, 93), although other molecules are assumed to pass through these high conductance channels (32, 33). Panx1-mediated ATP release has been associated with direct recruitment of inflammatory cells (39) or recruitment through P2X receptor–mediated pathways (41). Receptor signaling via P2X receptors is associated with increased processing of pro–IL-1β to its mature form and with IL-1β release (30, 31). Panx1-associated ATP release increases in caspase-1 and pro–IL-1β processing, promoting human gestational tissues (42). In astrocytes, Panx1-mediated ATP release and signaling through the P2X7 channel has been found to promote activation of the NLRP3 inflammasome and the release of IL-1β (43). Our results show that TNF-α treatments (2.5–100 ng/ml) of HUVECs resulted in the release of ∼10–20 nM ATP through Panx1 channels, which is similar to previous reports (94). In our study, we found that adding exogenous ATP (data not shown) or the stable ATP isoform (ATPγS) at these concentrations was not sufficient to stimulate IL-1β transcription. Nonetheless, previous studies found that nonphysiological levels of ATP (e.g., levels as high as 5 mM) induce IL-1β transcription, although these changes have been linked with cytotoxic effects of ATP at these concentrations (22–24, 26). In keeping with these observations, we found that treatment of HUVECs with 100 μM ATPγS did induce an increase IL-1β transcription that was inhibited by suramin, which has been found to effectively block P2X receptors at concentrations between 10 μM and 1 mM (44, 45). However, it should be noted that the ATP-induced IL-1β responses were significantly lower than those following TNF-α stimulation in our study. Furthermore, TNF-α–induced IL-1β and Panx1 expression in HUVECs was not altered by cotreatment with apyrase (to degrade ATP) or in the presence of suramin [nonspecific P2X/P2Y inhibition (45)] or A438079 hydrochloride [to block P2X7 receptors (45–47)]. Although it is possible that plasma membrane–localized release could produce a microenvironment of increased ATP concentrations surrounding purinergic receptors, our studies expressing a plasma membrane–bound luciferase demonstrated that TNF-α does not induces 100 μM ATP levels at the plasma membrane. Taken together, these data strongly suggest that ATP is not the primary mechanism for alterations in IL-1β synthesis in HUVECs following TNF-α treatment.

Panx1 channels are permeable to ions and molecules up to 1 kDa, and Vanden Abeele et al. (33) previously demonstrated that Panx1 channels in the endoplasmic reticulum facilitate the movement of Ca^{2+}. In this study, we found that $[Ca^{2+}]_i$ and transient Ca^{2+} waves are increased in HUVECs in response to TNF-α. Interestingly, this did not occur at earlier timepoints (5 hours), suggesting that kinase activation of TNF-α pathways is not involved. Rather, increases in $[Ca^{2+}]_i$ were only found after long-term stimulation of up to 24 hours, a timepoint at which we demonstrate Panx1 channels are functional at the plasma membrane. To assess the source of increased $[Ca^{2+}]_i$, we repeated TNF-α stimulation experiments in Ca^{2+}-free Krebs solution, which blocked the response, suggesting that increases in $[Ca^{2+}]_i$ originated from outside the cell. Although it is possible that other mechanisms serve to facilitate the entry of Ca^{2+} under these conditions, we provide several lines of evidence that suggest that Panx1 channels are directly permeable to Ca^{2+}, including no Ca^{2+} response to TNF-α when Panx1 is silenced by siRNA or the channel is inhibited using the Panx1-specific inhibitor peptide PxIL2P. Our data show that increases in $[Ca^{2+}]_i$ are associated with IL-1β -synthesis that can be ablated following reductions in $[Ca^{2+}]_i$ using EGTA-AM and by blocking the Panx1 channel. Our data therefore suggest that plasma membrane Panx1 channels are permeable to and facilitate increases in $[Ca^{2+}]_i$.

The NF-κB–p65 protein, is a downstream target of TNF-α signaling, and blocking its activation significantly alters TNF-α–associated gene regulation, including IL-1β (8). In this study, we have demonstrated that NF-κB activation plays a key role in early upregulation of Panx1 in ECs, which promotes its membrane trafficking and channel opening. Whereas Panx1 is a direct target

plus PxIL2P peptide (20 μM) treatment for 24 h ($n = 3$). (**F**) qRT-PCR analysis of IL-1β expression in HUVECs pretreated with PxIL2 peptide (20 μM) followed by TNF-α (2.5 ng/ml) plus PxIL2P peptide (20 μM) treatment for 24 h. Data were normalized to control and calculated to 2^-ΔΔCT, then expressed as fold change. Each group was performed in triplicates in addition to the technical triplicates ($n = 3$). (**G**) ELISA of IL-1β release from HUVECs following TNF-α treatment in the presence of PxIL2P (20 μM) or scrambled peptide (ScPep, 20 μM). Each measurement was performed in triplicate ($n = 3$). (**H**) Flow cytometric measurement of median $[Ca^{2+}]_i$ in HUVECs transfected with siPanx1 followed by TNF-α (2.5 ng/ml) stimulation ($n = 9$). (**I**) Flow cytometric measurement of median $[Ca^{2+}]_i$ in HUVECs treated with TNF-α for 24 h, then washed out for 8 d, as per experimental set up illustrated in Fig. 1C schematic. (**J**) qRT-PCR analysis of IL-1β expression in HUVECs treated with TNF-α for 24 h, then washed out for 8 d, as per experimental set up illustrated in Fig. 1C schematic. Data were normalized to control and calculated to 2^-ΔΔCT, then expressed as fold change. Each group was performed in triplicates in addition to the technical triplicates ($n = 3$). (**K**) Representative immunoblots of NF-κB–p65 (p65) and p-p65 HUVECs transfected with siControl or siRNA Panx1 for 48 h followed with 24-h TNF-α treatment (2.5 ng/ml) measured. β-tubulin was used as a loading control. The relative changes of p-p65 and p65 expression were calculated in comparison with siControl no treatment ($n = 3$). (**L**) Representative immunoblots of HUVECs pretreated with PxIL2P peptide followed with TNF-α (2.5 ng/ml) plus PxIL2P peptide (20 μM) stimulation for 24 h. β-tubulin was used as a loading control. The relative changes of P-65 and p65 expression were calculated in comparison with control no treatment ($n = 3$). Statistical analyses were performed by one-way or two-way ANOVA with either Dunnett or Tukey multiple comparison test. $^*p < 0.05$, $^{**}p < 0.01$, $^{***}p < 0.001$, $^{****}p < 0.001$. TNF, TNF-α.

Downloaded from http://www.jimmunol.org/ at Cochin Univ Biblio I894 on April 21, 2020

of NF-κB activation, we further demonstrate that Panx1 signaling can enhance NF-κB activation. This is in keeping with studies by Wu et al. (69) that pointed to a role of Panx1 in the control of NF-κB activation. Our data highlight that TNF-α induces an increase in p-p65 activation, that is significantly reduced when Panx1 expression is knocked down by siRNA and when the channel is blocked in the presence of the PxIL2P peptide. In vitro, our results do not lead to a complete reduction in IL-1β expression, which may suggest that the role of Panx1–Ca^{2+} signaling is to amplify the NF-κB–mediated responses through Ca^{2+}-mediated phosphorylation of p65, as previously described (68). Thus, we propose that Panx1 facilitates a feed-forward signaling through Ca^{2+}, leading to the transcriptional control of IL-1β.

Taken together, the results of our study highlight, to our knowledge, a novel reciprocal relationship between TNF-α and NF-κB signaling, which is regulated by Panx1 channel–mediated control of $[Ca^{2+}]_i$, leading to alterations in IL-1β synthesis and release by ECs.

Acknowledgments

We thank Anita Impagliazzo for illustration. The University of Virginia School of Medicine Flow Cytometry Facility was used for flow cytometric analysis. The University of Glasgow Polyomics core was used for RNA-seq, data interpretation, and analysis. We thank Dr. Graham Hamilton (Glasgow Polyomics) for input in experimental design and analysis of RNA-seq data. We thank Dr. Francesco Di Virgilio (University of Ferrara) for supply of the pmeLUC plasmid used in measurements of membrane ATP levels.

Disclosures

The authors have no financial conflicts of interest.

References

1. Libby, P., A. H. Lichtman, and G. K. Hansson. 2013. Immune effector mechanisms implicated in atherosclerosis: from mice to humans. [Published erratum appears in 2013 Immun*ity* 39: 413.] *Immunity* 38: 1092–1104.
2. Libby, P., and G. K. Hansson. 2015. Inflammation and immunity in diseases of the arterial tree: players and layers. *Circ. Res.* 116: 307–311.
3. Ridker, P. M. 2013. Closing the loop on inflammation and atherothrombosis: why perform the CIRT and CANTOS trials? *Trans. Am. Clin. Climatol. Assoc.* 124: 174–190.
4. Barath, P., M. C. Fishbein, J. Cao, J. Berenson, R. H. Helfant, and J. S. Forrester. 1990. Detection and localization of tumor necrosis factor in human atheroma. *Am. J. Cardiol.* 65: 297–302.
5. Ridker, P. M., N. Rifai, M. Pfeffer, F. Sacks, S. Lepage, and E. Braunwald. 2000. Elevation of tumor necrosis factor-alpha and increased risk of recurrent coronary events after myocardial infarction. *Circulation* 101: 2149–2153.
6. Bradley, J. R. 2008. TNF-mediated inflammatory disease. *J. Pathol.* 214: 149–160.
7. Imaizumi, T., H. Itaya, K. Fujita, D. Kudoh, S. Kudoh, K. Mori, K. Fujimoto, T. Matsumiya, H. Yoshida, and K. Satoh. 2000. Expression of tumor necrosis factor-alpha in cultured human endothelial cells stimulated with lipopolysaccharide or interleukin-1alpha. *Arterioscler. Thromb. Vasc. Biol.* 20: 410–415.
8. Perrot-Applanat, M., S. Vacher, A. Toullec, I. Pelaez, G. Velasco, F. Cormier, H. S. Saad, R. Lidereau, V. Baud, and I. Bièche. 2011. Similar NF-κB gene signatures in TNF-α treated human endothelial cells and breast tumor biopsies. *PLoS One* 6: e21589.
9. Viemann, D., M. Goebeler, S. Schmid, U. Nordhues, K. Klimmek, C. Sorg, and J. Roth. 2006. TNF induces distinct gene expression programs in microvascular and macrovascular human endothelial cells. *J. Leukoc. Biol.* 80: 174–185.
10. Alexander, M. R., C. W. Moehle, J. L. Johnson, Z. Yang, J. K. Lee, C. L. Jackson, and G. K. Owens. 2012. Genetic inactivation of IL-1 signaling enhances atherosclerotic plaque instability and reduces outward vessel remodeling in advanced atherosclerosis in mice. *J. Clin. Invest.* 122: 70–79.
11. Gabay, C., I. B. McInnes, A. Kavanaugh, K. Tuckwell, M. Klearman, J. Pulley, and N. Sattar. 2016. Comparison of lipid and lipid-associated cardiovascular risk marker changes after treatment with tocilizumab or adalimumab in patients with rheumatoid arthritis. *Ann. Rheum. Dis.* 75: 1806–1812.
12. Virone, A., J. P. Bastard, S. Fellahi, J. Capeau, S. Rouanet, J. Sibilia, P. Ravaud, F. Berenbaum, J. E. Gottenberg, and J. Sellam. 2019. Comparative effect of tumour necrosis factor inhibitors versus other biological agents on cardiovascular risk-associated biomarkers in patients with rheumatoid arthritis. *RMD Open* 5: e000897.
13. Di Minno, M. N., S. Iervolino, R. Peluso, R. Scarpa, and G. Di Minno, CaRRDs study group. 2011. Carotid intima-media thickness in psoriatic arthritis: differences between tumor necrosis factor-α blockers and traditional disease-modifying antirheumatic drugs. *Arterioscler. Thromb. Vasc. Biol.* 31: 705–712.
14. Ridker, P. M., C. P. Howard, V. Walter, B. Everett, P. Libby, J. Hensen, and T. Thuren, CANTOS Pilot Investigative Group. 2012. Effects of interleukin-1β inhibition with canakinumab on hemoglobin A1c, lipids, C-reactive protein, interleukin-6, and fibrinogen: a phase IIb randomized, placebo-controlled trial. *Circulation* 126: 2739–2748.
15. Solomon, D. H., R. J. Glynn, J. G. MacFadyen, P. Libby, T. Thuren, B. M. Everett, and P. M. Ridker. 2018. Relationship of interleukin-1β blockade with incident gout and serum uric acid levels: exploratory analysis of a randomized controlled trial. *Ann. Intern. Med.* 169: 535–542.
16. Ridker, P. M., B. M. Everett, T. Thuren, J. G. MacFadyen, W. H. Chang, C. Ballantyne, F. Fonseca, J. Nicolau, W. Koenig, S. D. Anker, et al; CANTOS Trial Group. 2017. Antiinflammatory therapy with canakinumab for atherosclerotic disease. *N. Engl. J. Med.* 377: 1119–1131.
17. Ridker, P. M., P. Libby, J. G. MacFadyen, T. Thuren, C. Ballantyne, F. Fonseca, W. Koenig, H. Shimokawa, B. M. Everett, and R. J. Glynn. 2018. Modulation of the interleukin-6 signalling pathway and incidence rates of atherosclerotic events and all-cause mortality: analyses from the Canakinumab Anti-Inflammatory Thrombosis Outcomes Study (CANTOS). *Eur. Heart J.* 39: 3499–3507.
18. Ridker, P. M., B. M. Everett, A. Pradhan, J. G. MacFadyen, D. H. Solomon, E. Zaharris, V. Mam, A. Hasan, Y. Rosenberg, E. Iturriaga, et al; CIRT Investigators. 2019. Low-dose methotrexate for the prevention of atherosclerotic events. *N. Engl. J. Med.* 380: 752–762.
19. Maître, B., S. Magnenat, V. Heim, C. Ravanat, R. J. Evans, H. de la Salle, C. Gachet, and B. Hechler. 2015. The P2X1 receptor is required for neutrophil extravasation during lipopolysaccharide-induced lethal endotoxemia in mice. *J. Immunol.* 194: 739–749.
20. Mariathasan, S., D. S. Weiss, K. Newton, J. McBride, K. O'Rourke, M. Roose-Girma, W. P. Lee, Y. Weinrauch, D. M. Monack, and V. M. Dixit. 2006. Cryopyrin activates the inflammasome in response to toxins and ATP. *Nature* 440: 228–232.
21. Qu, Y., S. Misaghi, K. Newton, L. L. Gilmour, S. Louie, J. E. Cupp, G. R. Dubyak, D. Hackos, and V. M. Dixit. 2011. Pannexin-1 is required for ATP release during apoptosis but not for inflammasome activation. *J. Immunol.* 186: 6553–6561.
22. Kanjanamekanant, K., P. Luckprom, and P. Pavasant. 2013. Mechanical stress-induced interleukin-1beta expression through adenosine triphosphate/P2X7 receptor activation in human periodontal ligament cells. *J. Periodontal Res.* 48: 169–176.
23. Mehta, V. B., J. Hart, and M. D. Wewers. 2001. ATP-stimulated release of interleukin (IL)-1beta and IL-18 requires priming by lipopolysaccharide and is independent of caspase-1 cleavage. *J. Biol. Chem.* 276: 3820–3826.
24. Cullen, S. P., C. J. Kearney, D. M. Clancy, and S. J. Martin. 2015. Diverse activators of the NLRP3 inflammasome promote IL-1β secretion by triggering necrosis. *Cell Rep.* 11: 1535–1548.
25. Jo, E. K., J. K. Kim, D. M. Shin, and C. Sasakawa. 2016. Molecular mechanisms regulating NLRP3 inflammasome activation. *Cell. Mol. Immunol.* 13: 148–159.
26. Stoffels, M., R. Zaal, N. Kok, J. W. van der Meer, C. A. Dinarello, and A. Simon. 2015. ATP-induced IL-1β specific secretion: true under stringent conditions. *Front. Immunol.* 6: 54.
27. Jantaratnotai, N., H. B. Choi, and J. G. McLarnon. 2009. ATP stimulates chemokine production via a store-operated calcium entry pathway in C6 glioma cells. *BMC Cancer* 9: 442.
28. Wilson, H. L., R. W. Varcoe, L. Stokes, K. L. Holland, S. E. Francis, S. K. Dower, A. Surprenant, and D. C. Crossman. 2007. P2X receptor characterization and IL-1/IL-1Ra release from human endothelial cells. *Br. J. Pharmacol.* 151: 115–127.
29. Yaron, J. R., S. Gangaraju, M. Y. Rao, X. Kong, L. Zhang, F. Su, Y. Tian, H. L. Glenn, and D. R. Meldrum. 2015. K(+) regulates Ca(2+) to drive inflammasome signaling: dynamic visualization of ion flux in live cells. *Cell Death Dis.* 6: e1954.
30. Brough, D., R. A. Le Feuvre, R. D. Wheeler, N. Solovyova, S. Hilfiker, N. J. Rothwell, and A. Verkhratsky. 2003. Ca2+ stores and Ca2+ entry differentially contribute to the release of IL-1 beta and IL-1 alpha from murine macrophages. *J. Immunol.* 170: 3029–3036.
31. Ainscough, J. S., G. F. Gerberick, I. Kimber, and R. J. Dearman. 2015. Interleukin-1β processing is dependent on a calcium-mediated interaction with calmodulin. *J. Biol. Chem.* 290: 31151–31161.
32. Chiu, Y. H., M. S. Schappe, B. N. Desai, and D. A. Bayliss. 2018. Revisiting multimodal activation and channel properties of Pannexin 1. *J. Gen. Physiol.* 150: 19–39.
33. Vanden Abeele, F., G. Bidaux, D. Gordienko, B. Beck, Y. V. Panchin, A. V. Baranova, D. V. Ivanov, R. Skryma, and N. Prevarskaya. 2006. Functional implications of calcium permeability of the channel formed by pannexin 1. *J. Cell Biol.* 174: 535–546.
34. Michalski, K., J. L. Syrjanen, E. Henze, J. Kumpf, H. Furukawa, and T. Kawate. 2020. The Cryo-EM structure of pannexin 1 reveals unique motifs for ion selection and inhibition. *Elife*. DOI: 10.7554/eLife.54670.
35. Chekeni, F. B., M. R. Elliott, J. K. Sandilos, S. F. Walk, J. M. Kinchen, E. R. Lazarowski, A. J. Armstrong, S. Penuela, D. W. Laird, G. S. Salvesen, et al. 2010. Pannexin 1 channels mediate 'find-me' signal release and membrane permeability during apoptosis. *Nature* 467: 863–867.
36. Thompson, R. J., M. F. Jackson, M. E. Olah, R. L. Rungta, D. J. Hines, M. A. Beazely, J. F. MacDonald, and B. A. MacVicar. 2008. Activation of pannexin-1 hemichannels augments aberrant bursting in the hippocampus. *Science* 322: 1555–1559.

Downloaded from http://www.jimmunol.org/ at Cochin Univ Biblio I894 on April 21, 2020

37. Orellana, J. A., N. Froger, P. Ezan, J. X. Jiang, M. V. Bennett, C. C. Naus, C. Giaume, and J. C. Sáez. 2011. ATP and glutamate released via astroglial connexin 43 hemichannels mediate neuronal death through activation of pannexin 1 hemichannels. *J. Neurochem.* 118: 826–840.
38. Billaud, M., A. W. Lohman, A. C. Straub, R. Looft-Wilson, S. R. Johnstone, C. A. Araj, A. K. Best, F. B. Chekeni, K. S. Ravichandran, S. Penuela, et al. 2011. Pannexin1 regulates α1-adrenergic receptor- mediated vasoconstriction. *Circ. Res.* 109: 80–85.
39. Lohman, A. W., I. L. Leskov, J. T. Butcher, S. R. Johnstone, T. A. Stokes, D. Begandt, L. J. DeLalio, A. K. Best, S. Penuela, N. Leitinger, et al. 2015. Pannexin 1 channels regulate leukocyte emigration through the venous endothelium during acute inflammation. *Nat. Commun.* 6: 7965.
40. Good, M. E., S. A. Eucker, J. Li, H. M. Bacon, S. M. Lang, J. T. Butcher, T. J. Johnson, R. P. Gaykema, M. K. Patel, Z. Zuo, and B. E. Isakson. 2018. Endothelial cell Pannexin1 modulates severity of ischemic stroke by regulating cerebral inflammation and myogenic tone. *JCI Insight*. DOI: 10.1172/jci.insight.96272.
41. Pelegrin, P. 2008. Targeting interleukin-1 signaling in chronic inflammation: focus on P2X(7) receptor and Pannexin-1. *Drug News Perspect.* 21: 424–433.
42. Lappas, M. 2014. Caspase-1 activation is increased with human labour in foetal membranes and myometrium and mediates infection-induced interleukin-1β secretion. *Am. J. Reprod. Immunol.* 71: 189–201.
43. Albalawi, F., W. Lu, J. M. Beckel, J. C. Lim, S. A. McCaughey, and C. H. Mitchell. 2017. The P2X7 receptor primes IL-1β and the NLRP3 inflammasome in astrocytes exposed to mechanical strain. *Front. Cell. Neurosci.* 11: 227.
44. Hoyle, C. H., G. E. Knight, and G. Burnstock. 1990. Suramin antagonizes responses to P2-purinoceptor agonists and purinergic nerve stimulation in the guinea-pig urinary bladder and taenia coli. *Br. J. Pharmacol.* 99: 617–621.
45. Draganov, D., S. Gopalakrishna-Pillai, Y. R. Chen, N. Zuckerman, S. Moeller, C. Wang, D. Ann, and P. P. Lee. 2015. Modulation of P2X4/P2X7/Pannexin-1 sensitivity to extracellular ATP via Ivermectin induces a non-apoptotic and inflammatory form of cancer cell death. *Sci. Rep.* 5: 16222.
46. Karmakar, M., M. A. Katsnelson, G. R. Dubyak, and E. Pearlman. 2016. Neutrophil P2X7 receptors mediate NLRP3 inflammasome-dependent IL-1β secretion in response to ATP. *Nat. Commun.* 7: 10555.
47. Jiang, W., M. Li, F. He, S. Zhou, and L. Zhu. 2017. Targeting the NLRP3 inflammasome to attenuate spinal cord injury in mice. *J. Neuroinflammation* 14: 207.
48. Kishore, N., C. Sommers, S. Mathialagan, J. Guzova, M. Yao, S. Hauser, K. Huynh, S. Bonar, C. Mielke, L. Albee, et al. 2003. A selective IKK-2 inhibitor blocks NF-kappa B-dependent gene expression in interleukin-1 beta-stimulated synovial fibroblasts. *J. Biol. Chem.* 278: 32861–32871.
49. Vigont, V. A., O. A. Zimina, L. N. Glushankova, I. B. Bezprozvanny, G. N. Mozhayeva, and E. Kaznacheyeva. 2012. Store-operated calcium entry into SK-N-SH human neuroblastoma cells modeling huntington's disease. *Biochem. Moscow Suppl. Ser. A* 6: 206–214.
50. Adhikary, G., Y. Sun, and E. Pearlman. 2008. C-Jun NH2 terminal kinase (JNK) is an essential mediator of toll-like receptor 2-induced corneal inflammation. *J. Leukoc. Biol.* 83: 991–997.
51. Billaud, M., Y. H. Chiu, A. W. Lohman, T. Parpaite, J. T. Butcher, S. M. Mutchler, L. J. DeLalio, M. V. Artamonov, J. K. Sandilos, A. K. Best, et al. 2015. A molecular signature in the pannexin1 intracellular loop confers channel activation by the α1 adrenoreceptor in smooth muscle cells. *Sci. Signal.* 8: ra17.
52. Good, M. E., Y. H. Chiu, I. K. H. Poon, C. B. Medina, J. T. Butcher, S. K. Mendu, L. J. DeLalio, A. W. Lohman, N. Leitinger, E. Barrett, et al. 2018. Pannexin 1 channels as an unexpected new target of the anti-hypertensive drug spironolactone. *Circ. Res.* 122: 606–615.
53. Pellegatti, P., S. Falzoni, P. Pinton, R. Rizzuto, and F. Di Virgilio. 2005. A novel recombinant plasma membrane-targeted luciferase reveals a new pathway for ATP secretion. *Mol. Biol. Cell* 16: 3659–3665.
54. Vines, A., G. J. McBean, and A. Blanco-Fernández. 2010. A flow-cytometric method for continuous measurement of intracellular Ca(2+) concentration. *Cytometry A* 77: 1091–1097.
55. Lock, J. T., I. Parker, and I. F. Smith. 2015. A comparison of fluorescent Ca^{+} indicators for imaging local Ca^{+} signals in cultured cells. *Cell Calcium* 58: 638–648.
56. Moncoq, K., C. A. Trieber, and H. S. Young. 2007. The molecular basis for cyclopiazonic acid inhibition of the sarcoplasmic reticulum calcium pump. *J. Biol. Chem.* 282: 9748–9757.
57. Ottolini, M., K. Hong, E. L. Cope, Z. Daneva, L. J. DeLalio, J. D. Sokolowski, C. Marziano, N. Y. Nguyen, J. Altschmied, J. Haendeler, et al. 2020. Local peroxynitrite impairs endothelial TRPV4 channels and elevates blood pressure in obesity. *Circulation* DOI: 10.1161/CIRCULATIONAHA.119.043385.
58. Penuela, S., R. Bhalla, X. Q. Gong, K. N. Cowan, S. J. Celetti, B. J. Cowan, D. Bai, Q. Shao, and D. W. Laird. 2007. Pannexin 1 and pannexin 3 are glycoproteins that exhibit many distinct characteristics from the connexin family of gap junction proteins. *J. Cell Sci.* 120: 3772–3783.
59. Penuela, S., S. J. Celetti, R. Bhalla, Q. Shao, and D. W. Laird. 2008. Diverse subcellular distribution profiles of pannexin 1 and pannexin 3. *Cell Commun. Adhes.* 15: 133–142.
60. Boassa, D., C. Ambrosi, F. Qiu, G. Dahl, G. Gaietta, and G. Sosinsky. 2007. Pannexin1 channels contain a glycosylation site that targets the hexamer to the plasma membrane. *J. Biol. Chem.* 282: 31733–31743.
61. Zhou, P., S. Lu, Y. Luo, S. Wang, K. Yang, Y. Zhai, G. Sun, and X. Sun. 2017. Attenuation of TNF-α-induced inflammatory injury in endothelial cells by ginsenoside Rb1 via inhibiting NF-κB, JNK and p38 signaling pathways. *Front. Pharmacol.* 8: 464.
62. Sharma, A. K., E. J. Charles, Y. Zhao, A. K. Narahari, P. K. Baderdinni, M. E. Good, U. M. Lorenz, I. L. Kron, D. A. Bayliss, K. S. Ravichandran, et al. 2018. Pannexin-1 channels on endothelial cells mediate vascular inflammation during lung ischemia-reperfusion injury. *Am. J. Physiol. Lung Cell. Mol. Physiol.* 315: L301–L312.
63. Chen, K. W., B. Demarco, and P. Broz. 2020. Pannexin-1 promotes NLRP3 activation during apoptosis but is dispensable for canonical or noncanonical inflammasome activation. *Eur. J. Immunol.* 50: 170–177.
64. Ridker, P. M. 2019. Anti-inflammatory therapy for atherosclerosis: interpreting divergent results from the CANTOS and CIRT clinical trials. *J. Intern. Med.* 285: 503–509.
65. Dinarello, C. A. 2010. Anti-inflammatory agents: present and future. *Cell* 140: 935–950.
66. Brown, W. V., A. T. Remaley, and P. M. Ridker. 2015. JCL Roundtable: is inflammation a future target in preventing arteriosclerotic cardiovascular disease. *J. Clin. Lipidol.* 9: 119–128.
67. Penuela, S., R. Gehi, and D. W. Laird. 2013. The biochemistry and function of pannexin channels. *Biochim. Biophys. Acta* 1828: 15–22.
68. Martin, A. G., B. San-Antonio, and M. Fresno. 2001. Regulation of nuclear factor kappa B transactivation. Implication of phosphatidylinositol 3-kinase and protein kinase C zeta in c-Rel activation by tumor necrosis factor alpha. *J. Biol. Chem.* 276: 15840–15849.
69. Wu, L. Y., Z. N. Ye, C. H. Zhou, C. X. Wang, G. B. Xie, X. S. Zhang, Y. Y. Gao, Z. H. Zhang, M. L. Zhou, Z. Zhuang, et al. 2017. Roles of pannexin-1 channels in inflammatory response through the TLRs/NF-Kappa B signaling pathway following experimental subarachnoid hemorrhage in rats. *Front. Mol. Neurosci.* 10: 175.
70. Warner, S. J., and P. Libby. 1989. Human vascular smooth muscle cells. Target for and source of tumor necrosis factor. *J. Immunol.* 142: 100–109.
71. Jean-Charles, P. Y., J. H. Wu, L. Zhang, S. Kaur, I. Nepliouev, J. A. Stiber, L. Brian, R. Qi, V. Wertman, S. K. Shenoy, and N. J. Freedman. 2018. USP20 (ubiquitin-specific protease 20) inhibits TNF (tumor necrosis factor)-triggered smooth muscle cell inflammation and attenuates atherosclerosis. *Arterioscler. Thromb. Vasc. Biol.* 38: 2295–2305.
72. Gane, J. M., R. A. Stockley, and E. Sapey. 2016. TNF-α autocrine feedback loops in human monocytes: the pro- and anti-inflammatory roles of the TNF-α receptors support the concept of selective TNFR1 blockade *in vivo*. *J. Immunol. Res.* 2016: 1079851.
73. Boyce, A. K. J., A. L. Epp, A. Nagarajan, and L. A. Swayne. 2018. Transcriptional and post-translational regulation of pannexins. *Biochim. Biophys. Acta Biomembr.* 1860: 72–82.
74. Jiang, T., R. X. Xu, A. W. Zhang, W. Di, Z. J. Xiao, J. Y. Miao, N. Luo, and Y. N. Fang. 2012. Effects of transcranial direct current stimulation on hemichannel pannexin-1 and neural plasticity in rat model of cerebral infarction. *Neuroscience* 226: 421–426.
75. Bokhari, F. A., T. A. Shakoori, A. Butt, and F. Ghafoor. 2014. TNF-alpha: a risk factor for ischemic stroke. *J. Ayub Med. Coll. Abbottabad* 26: 111–114.
76. Tuttolomondo, A., R. Pecoraro, and A. Pinto. 2014. Studies of selective TNF inhibitors in the treatment of brain injury from stroke and trauma: a review of the evidence to date. *Drug Des. Devel. Ther.* 8: 2221–2238.
77. Liu, F., and L. D. McCullough. 2011. Middle cerebral artery occlusion model in rodents: methods and potential pitfalls. *J. Biomed. Biotechnol.* 2011: 464701.
78. Tuttolomondo, A., R. Di Sciacca, D. Di Raimondo, C. Renda, A. Pinto, and G. Licata. 2009. Inflammation as a therapeutic target in acute ischemic stroke treatment. *Curr. Top. Med. Chem.* 9: 1240–1260.
79. Dufresne, J., and D. G. Cyr. 2014. Regulation of the pannexin-1 promoter in the rat epididymis. *Biol. Reprod.* 91: 143.
80. Tobe, M., Y. Isobe, H. Tomizawa, T. Nagasaki, H. Takahashi, T. Fukazawa, and H. Hayashi. 2003. Discovery of quinazolines as a novel structural class of potent inhibitors of NF-kappa B activation. *Bioorg. Med. Chem.* 11: 383–391.
81. Gong, K., G. Guo, D. E. Gerber, B. Gao, M. Peyton, C. Huang, J. D. Minna, K. J. Hatanpaa, K. Kernstine, L. Cai, et al. 2018. TNF-driven adaptive response mediates resistance to EGFR inhibition in lung cancer. *J. Clin. Invest.* 128: 2500–2518.
82. Laird, D. W., C. C. Naus, and P. D. Lampe. 2017. SnapShot: connexins and disease. *Cell* 170: 1260–1260.e1.
83. Laird, D. W. 2006. Life cycle of connexins in health and disease. *Biochem. J.* 394: 527–543.
84. Boassa, D., F. Qiu, G. Dahl, and G. Sosinsky. 2008. Trafficking dynamics of glycosylated pannexin 1 proteins. *Cell Commun. Adhes.* 15: 119–132.
85. DeLalio, L. J., M. Billaud, C. A. Ruddiman, S. R. Johnstone, J. T. Butcher, A. G. Wolpe, X. Jin, T. C. S. Keller, IV, A. S. Keller, T. Rivière, et al. 2019. Constitutive SRC-mediated phosphorylation of pannexin 1 at tyrosine 198 occurs at the plasma membrane. *J. Biol. Chem.* 294: 6940–6956.
86. Everett, B. M., A. D. Pradhan, D. H. Solomon, N. Paynter, J. Macfadyen, E. Zaharris, M. Gupta, M. Clearfield, P. Libby, A. A. Hasan, et al. 2013. Rationale and design of the cardiovascular inflammation reduction trial: a test of the inflammatory hypothesis of atherothrombosis. *Am Heart J* 166: 199–207.e15.
87. Cronstein, B. N., D. Naime, and E. Ostad. 1993. The antiinflammatory mechanism of methotrexate. Increased adenosine release at inflamed sites diminishes leukocyte accumulation in an in vivo model of inflammation. *J. Clin. Invest.* 92: 2675–2682.
88. Chan, E. S., and B. N. Cronstein. 2010. Methotrexate--how does it really work? *Nat. Rev. Rheumatol.* 6: 175–178.
89. Zernecke, A., E. Shagdarsuren, and C. Weber. 2008. Chemokines in atherosclerosis: an update. *Arterioscler. Thromb. Vasc. Biol.* 28: 1897–1908.

Downloaded from http://www.jimmunol.org/ at Cochin Univ Biblio I894 on April 21, 2020

90. Szentes, V., M. Gazdag, I. Szokodi, and C. A. Dézsi. 2018. The role of CXCR3 and associated chemokines in the development of atherosclerosis and during myocardial infarction. *Front. Immunol.* 9: 1932.
91. Segers, D., J. A. Lipton, P. J. Leenen, C. Cheng, D. Tempel, G. Pasterkamp, F. L. Moll, R. de Crom, and R. Krams. 2011. Atherosclerotic plaque stability is affected by the chemokine CXCL10 in both mice and humans. *Int. J. Inflamm.* 2011: 936109.
92. Heller, E. A., E. Liu, A. M. Tager, Q. Yuan, A. Y. Lin, N. Ahluwalia, K. Jones, S. L. Koehn, V. M. Lok, E. Aikawa, et al. 2006. Chemokine CXCL10 promotes atherogenesis by modulating the local balance of effector and regulatory T cells. *Circulation* 113: 2301–2312.
93. Romanov, R. A., M. F. Bystrova, O. A. Rogachevskaya, V. B. Sadovnikov, V. I. Shestopalov, and S. S. Kolesnikov. 2012. The ATP permeability of pannexin 1 channels in a heterologous system and in mammalian taste cells is dispensable. *J. Cell Sci.* 125: 5514–5523.
94. Tozzi, M., J. B. Hansen, and I. Novak. 2020. Pannexin-1 mediated ATP release in adipocytes is sensitive to glucose and insulin and modulates lipolysis and macrophage migration. *Acta Physiol. (Oxf.)* 228: e13360.

Downloaded from http://www.jimmunol.org/ at Cochin Univ Biblio I894 on April 21, 2020